



# Synthesis and characterization of Pd<sup>0</sup> nanoparticles supported over hydroxyapatite nanospheres for potential application as a promising catalyst for nitrophenol reduction

Adem Rüzgar<sup>\*\*</sup>, Yaşar Karataş, Mehmet Gülcan<sup>\*,1</sup>

Department of Chemistry, Van Yüziüncü Yıl University, Van, 65080, Turkey

## ARTICLE INFO

### Keywords:

Hydroxyapatite  
Nanoparticles  
Nitrophenols  
Palladium  
Reduction

## ABSTRACT

Nitrophenols, which are defined as an important toxic and carcinogenic pollutant in agricultural and industrial wastewater due to their solubility in water, form of resistance against all organisms in water resources. It is vital that these compounds, which are highly toxic as well as highly explosive, are removed from the aquatic ecosystem. In this paper, we reported the preparation and advanced characterization of Pd<sup>0</sup> nanoparticles supported over hydroxyapatite nanospheres (Pd<sup>0</sup>@nano-HAp). The catalytic efficiency of the Pd<sup>0</sup>@nano-HAp catalyst was examined in the reduction of nitrophenols in water in the presence of NaBH<sub>4</sub> as reducing agent and the great activity of catalyst have been specified against 2-nitrophenol, 4-nitrophenol, 2,4-dinitrophenol and 2,4,6-trinitrophenol compounds with 70.6, 82.4, 27.6 and 41.4 min<sup>-1</sup> TOF<sub>initial</sub> values, respectively. Another important point is that the Pd<sup>0</sup>@nano-HAp catalyst has perfect reusability performance (at 5th reuse between 68.5 and 92.8 %) for the reduction of nitrophenols. In addition, catalytic studies were carried out at different temperatures in order to determine thermodynamic parameters such as  $E_a$ ,  $\Delta H^\ddagger$  and  $\Delta S^\ddagger$ .

## 1. Introduction

The rapidly increasing world population and urbanization in the last century have resulted in critical processes that support each other in the form of “more production”, “more consumption” and “more waste” in almost every field, especially in industry and agriculture. Organic and inorganic pollutants released by the effect of these processes can cause serious and permanent damage to both surface waters such as seas, lakes, streams and underground waters. Nitrophenols, which are extremely effective even at very low concentrations, are among the most dangerous and harmful chemicals. Due to their toxicity and carcinogenic nature, nitrophenols are considered in the group of compounds that need to be purified primarily [1–5].

In general, many studies are carried out on the purification of nitrophenol compounds, which have serious negative effects on all ecosystems and living creatures in these ecosystems that are directly or indirectly affected by water resources. In these studies, many methods are tried in which different physical and chemical parameters are tested [6–8]. However, most of these methods cannot adequately meet the needs due to their long duration, low efficiency, high cost and application difficulties. For this reason, researchers

\* Corresponding author.

\*\* Corresponding author.

E-mail addresses: [aruzgar@yyu.edu.tr](mailto:aruzgar@yyu.edu.tr) (A. Rüzgar), [mehmetgulcan65@gmail.com](mailto:mehmetgulcan65@gmail.com) (M. Gülcan).

<sup>1</sup> <http://avesis.yyu.edu.tr/mehmetgulcan>.

have focused on developing new methods and techniques that are highly effective, environmentally friendly and applicable. The data obtained from the studies revealed that the catalytic hydrogenation process, in which the  $\text{NO}_2$  group in nitrophenol derivatives is converted to  $\text{NH}_2$ , is a very effective method. The main features that make this method preferable are cost, efficiency, time, applicability and high conversion efficiency. Another advantage of this method is that aminophenols obtained as a result of reduction they have much lower toxicity than nitrophenols. It is known that aminophenols are widely used in pesticide, medicine, paint, paper production and cosmetics industries. In addition, aminophenol derivatives are needed as intermediates in the synthesis process of paracetamol, which is an important drug active ingredient and is widely used today [9]. In conclusion, as a result of the application of the catalytic hydrogenation method, which is widely used in the pharmaceutical, petrochemical, and food industries, to nitrophenols, on one hand, nitrophenols, which are extremely dangerous chemicals in terms of human health every aspect, can be purified/converted economically and environmentally; On the other hand, it is possible to obtain aminophenols, which are needed in many industrial production processes and considered as very important intermediate products [10,11].

One of the critical steps in converting nitrophenols to aminophenols, which are much less harmful compounds, is to identify a suitable hydrogen source. Although different hydrogen sources are encountered in the literature,  $\text{NaBH}_4$  is mostly used as a reducing agent because of its advantages such as being economical and environmentally friendly, easy to store, and high solubility in water and alcohol [12–19]. Despite all these advantages, if  $\text{NaBH}_4$  is used alone in the reduction process, the reaction takes place very slowly, causing time and energy loss. Research-application studies have revealed that these problems encountered in the case of using  $\text{NaBH}_4$  alone can be eliminated with efficient catalyst (metal-support) systems. In this context, it has been reported that catalyst systems obtained from solid supported metal nanoparticles both accelerate the hydrolysis of  $\text{NaBH}_4$  and provide high reusability performance in the reduction of nitrophenols to aminophenols by preventing aggregation of active metal nanoparticles [20–31].

Metal oxides, metal-organic frameworks, carbon-based materials, and polymeric structures are the leading support materials used to better both the catalytic effectiveness and reusability performance and to eliminate the negativities caused by the aggregation of active metal nanoparticles. Among these materials, carbon nanofibers, carbon nanotubes and graphene derivatives have been at the center of many researches due to their interesting physicochemical properties and durability. The data obtained from the studies revealed that these materials, which are used as supports, significantly increase the efficiency and stability of nanocatalysts [32–39]. In recent years, unlike these support materials, apatites, which are in the group of bioceramic materials, have started to attract the attention of scientists due to their chemical properties and robustness. Hydroxyapatite (HAp;  $[\text{Ca}_{10}(\text{PO}_4)_6(\text{OH})_2]$ ), an important member of the apatites, has become one of the prominent materials with its large surface area, very high adsorption potential and excellent biocompatibility. Other features that make HAp, which is accepted as a member of the structurally and chemically less soluble calcium phosphate salts family, more advantageous than similar support materials, can be listed as its high ion exchange capability and low surface acidity that eliminates unwanted side reactions [40–46].

HAp; it has a crystal structure containing polyatomic ions such as calcium, phosphate and hydroxyl. This crystal structure makes it easy to add different elements and groups to HAp and to change the structure. Having such a chemical structure of HAp allows it to be decorated with many functional materials such as metals, metal oxides and polymers [47–49] (Scheme 1).

HAp, which is used in a wide range of fields from medicine to metallurgy, from bioengineering to chemistry, can be synthesized by different methods such as biomineralization, solid state, emulsion, reverse micelle, electrochemical application, sol-gel, aqueous colloidal precipitation, direct spraying and hydration [50–57]. Different metals such as Pd (0) [58], Ru (0) [59,60], Ag (0) [61–63], Au (0) [64], Cu [65], and Ni [66] were used in the catalyst systems in which HAp is applied as a support material, and it has been reported that the obtained nanoparticles perform quite well. Catalysts obtained as a result of the use of HAp as a support material; it has been used in selective oxidation of alcohols [58], Suzuki-Miyaura cross-coupling reactions [67], partial oxidation of hydrocarbons, hydrogenation of furfural derivatives [68], selective reduction of unsaturated ketones [69]. In addition, HAp supported nanoparticles were used in the production of hydrogen from hydrogen sources such as ammonia-borane and sodium borohydride [70].

Nanoparticles (NPs), which are also expressed as submicron molecules consisting of organic or inorganic materials, show more effective and fascinating properties than bulk materials due to their size-dependent properties. The variety of materials used in the synthesis of NPs has enabled the researchers to prepare species with different compositions and morphologies NPs such as metallic, semiconductor, metal and non-metal oxides, and carbon [71]. So far, Pd/GNS- $\text{NH}_2$  [6], Ni-NP/ENF [72], Au NPs/AC [73], Ag NPs-PG [74], Fe@NC@Pd [75], RGO@AC/Pd [76], Pd@ASNTs [77], NCT@Pd [78], CMF@PDA/Pd [79], PDA-g- $\text{C}_3\text{N}_4$ /Au [80], DPNS [81], COF-TPCBP [82], Pd-Cu@Noria-GO [83], MgAl-LDH [84], Ag-CeO<sub>2</sub> [85], Fe-N-C [86], Au/Pd-loaded yeast [87], Pd<sub>1</sub>@np-Ni/NiO [88] and AuNS-MoS<sub>2</sub> QDs [89] catalysts have been developed for the reduction of nitrophenols in cooperation with  $\text{NaBH}_4$ .

In this study, hydroxyapatite nanospheres (*nano*-HAp) supported palladium (0) nanoparticles were prepared (hereafter named as Pd<sup>0</sup>@*nano*-HAp) in order to reduce the nitrophenols to aminophenols in an efficient, environmentally friendly and feasible way. In studies where  $\text{NaBH}_4$  was used as a reducing agent, catalytic reduction processes were investigated kinetic and thermodynamically at different temperature. The structure of the prepared Pd<sup>0</sup>@*nano*-HAp catalyst was characterized in detail by spectroscopic tools such as ICP-OES, *P*-XRD, XPS, TEM, HR-TEM, EDX, SEM and BET surface area techniques. The results obtained can be summarized as follows: (i) The catalytic effectiveness of Pd<sup>0</sup>@*nano*-HAp catalyst in reduction of nitrophenols is extremely high (TOF<sub>initial</sub> values: 70.6 min<sup>-1</sup> for 2-NP, 82.4 min<sup>-1</sup> for 4-NP, 27.6 min<sup>-1</sup> for 2,4-DNP and 41.4 min<sup>-1</sup> for 2,4,6-TNP), (ii) HAp, used as a solid support material, both facilitates the kinetic control of the catalytic reaction and greatly inhibits undesirable processes such as aggregation, which reduces the activity and shortens the catalyst life, (iii) The reusability performance of Pd<sup>0</sup>@*nano*-HAp catalyst in the catalytic reduction is quite high.

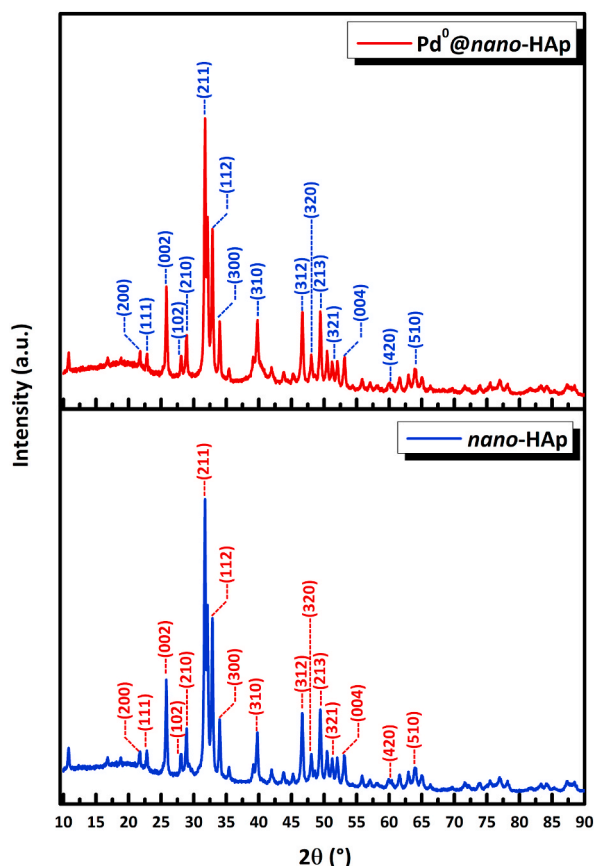


Fig. 1. P-XRD patterns of *nano-HAp* and  $\text{Pd}^0@nano\text{-HAp}$  catalyst obtained under *in-situ* conditions from the reduction of 4-NP in the  $2\theta$  range of  $10\text{--}90^\circ$ .

## 2. Experimental

### 2.1. Materials

Palladium nitrate hydrate ( $\text{Pd}(\text{NO}_3)_2 \cdot x\text{H}_2\text{O}$ ), hydroxyapatite ( $[\text{Ca}_5(\text{OH})(\text{PO}_4)_3]_x$ , nanopowder,  $<200$  nm particle size,  $\geq 97\%$ , HAp), sodium borohydride ( $\text{NaBH}_4$ , powder,  $\geq 98.0\%$ ), 2-nitrophenol ( $\text{O}_2\text{NC}_6\text{H}_4\text{OH}$ , 98 %, 2-NP), 4-nitrophenol (*p*-nitrophenol,  $\text{O}_2\text{NC}_6\text{H}_4\text{OH}$ ,  $\geq 99\%$ , 4-NP), 2,4-dinitrophenol ( $\alpha$ -dinitrophenol,  $(\text{O}_2\text{N})_2\text{C}_6\text{H}_3\text{OH}$ ,  $\geq 98.0\%$ , 2,4-DNP), and 2,4,6-nitrophenol (picric acid,  $(\text{O}_2\text{N})_3\text{C}_6\text{H}_2\text{OH}$ ,  $\geq 98\%$ ) were supplied from Sigma-Aldrich®.

### 2.2. *In-situ* formation of $\text{Pd}^0@nano\text{-HAp}$ catalyst and its catalytic activity in the nitrophenol reduction

Experimental procedures related to the investigation of both the  $\text{Pd}^0@nano\text{-HAp}$  catalyst synthesized *in-situ* conditions and the catalytic performances of the obtained catalyst in the reduction of nitrophenol derivatives [6,72] are presented as Supplementary Material.

### 2.3. Characterization tools of $\text{Pd}^0@nano\text{-HAp}$ catalyst

This part is given in the Supplementary Material.

### 2.4. Investigation of reusability performance of $\text{Pd}^0@nano\text{-HAp}$ catalyst in the nitrophenol reduction

After the conversion of the nitro group in the aromatic ring to the amine group was completed as a result of catalytic reduction, the HAp catalyst was filtered and washed with the appropriate solvent mixture. The pure catalyst was dried under vacuum at 353 K and made ready for reuse. After weighing the amount of catalyst to be used, catalytic hydrogenation was restarted with the targeted nitrophenol derivative.

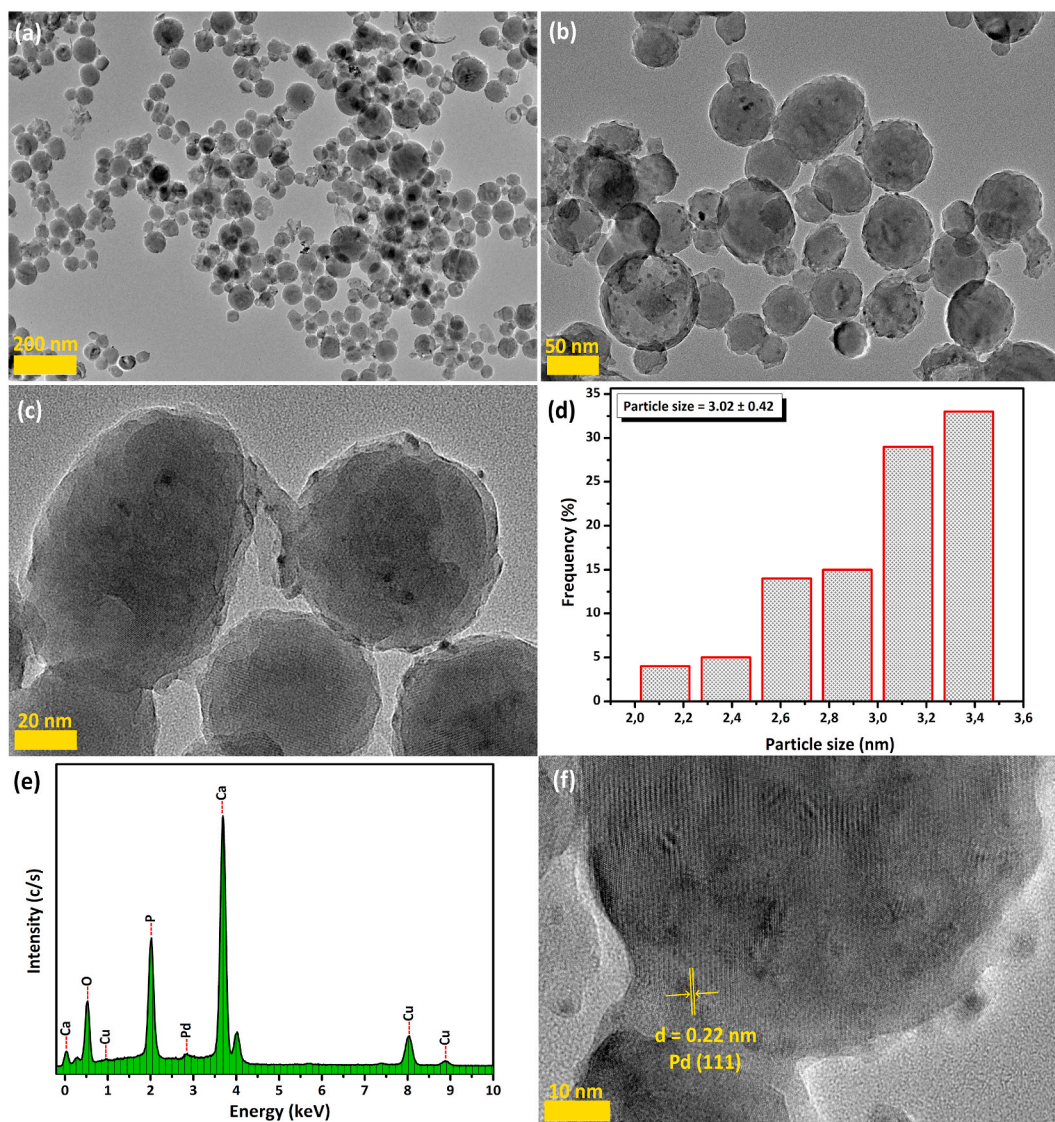


**Fig. 2.** TEM images in different scale (a–c), corresponding particle size histogram (d), TEM/EDX spectrum (e), and HR-TEM image (f) of Pd<sup>0</sup>@nano-HAp catalyst obtained under *in-situ* conditions from the reduction of 4-NP.

### 2.5. The activation parameters for Pd<sup>0</sup>@nano-HAp catalyst in the nitrophenol reduction

For the calculation of  $E_a$ ,  $\Delta H^\ddagger$  and  $\Delta S^\ddagger$  in each experiment, 5 mg (1.24 wt% Pd, 0.58  $\mu\text{mol}$ ) of Pd<sup>0</sup>@nano-HAp and 2.0 mM (20  $\mu\text{mol}$ ) aqueous solution (10 mL) of the NP derivatives (2-NP: 2.78 mg, 4-NP: 2.78 mg, 2,4-DNP: 3.68 mg and 2,4,6-TNP: 4.58 mg) were taken in a jacketed Schlenk. Depending on the initial rate, Arrhenius and Eyring-Polanyi graphs were drawn and  $E_a$ ,  $\Delta H^\ddagger$  and  $\Delta S^\ddagger$  parameters were calculated by catalytic experiments performed at temperatures between 298 and 318 K.

## 3. Results and discussion

### 3.1. Characterization of Pd<sup>0</sup>@nano-HAp catalyst

*P*-XRD patterns of Pd<sup>0</sup>@nano-HAp catalyst and nano-HAp formed under *in-situ* conditions as a result of catalytic reduction of 4-NP are given in Fig. 1. The presence of strong diffraction peaks observed in the patterns indicates that the samples are highly crystalline (nano-HAp, JCPDS file no. 00-009-0432). In addition, when the expanded structure of the diffraction peaks is examined, it is clearly understood that the grain sizes of the sample are in the nanometer scale [90]. The compared *P*-XRD patterns reveal that there is no observable change in the crystallinity of nano-HAp during the reduction of Pd<sup>2+</sup> ions to Pd<sup>0</sup> in the nano-HAp matrix. In addition, partial

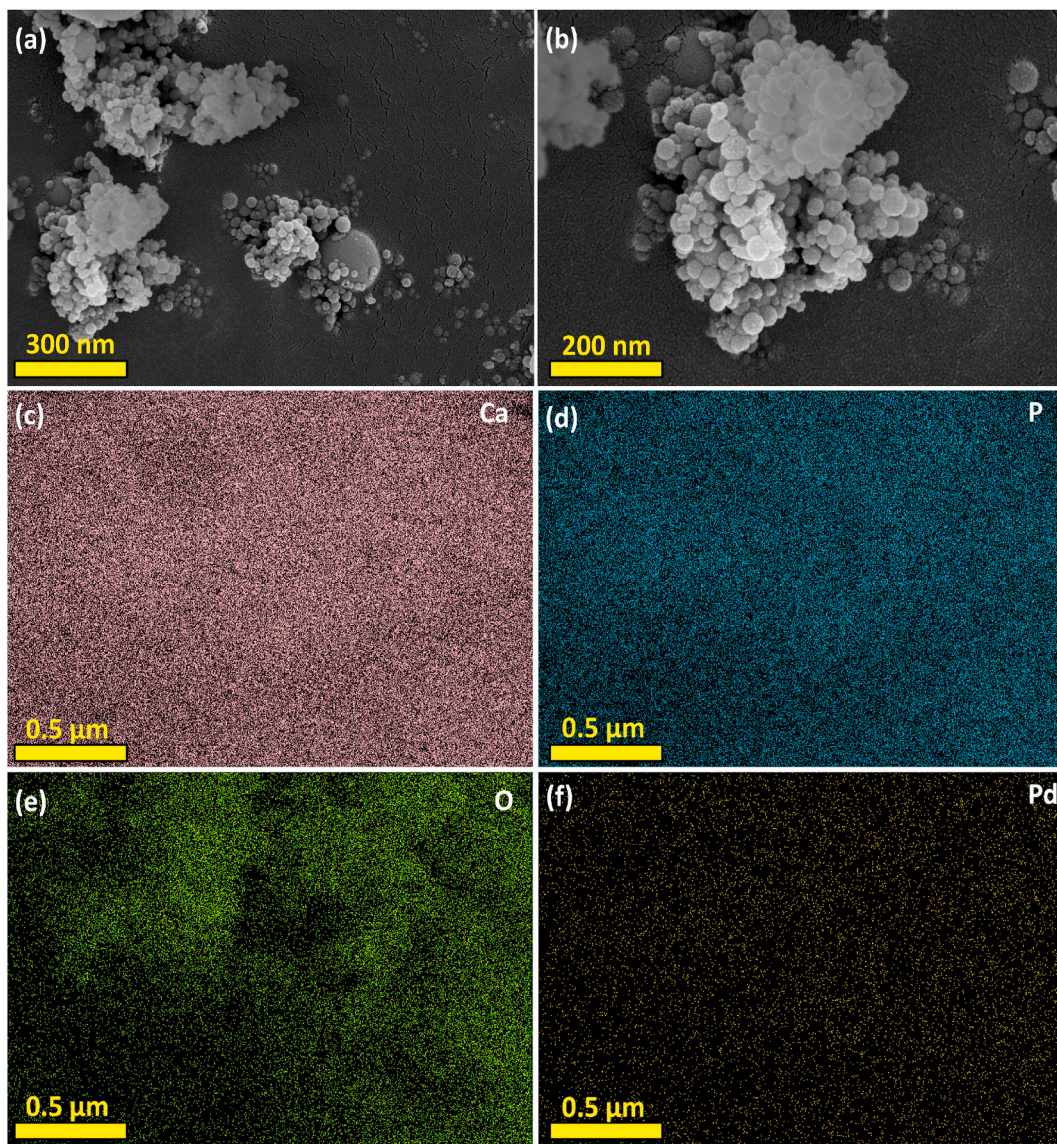


**Fig. 3.** SEM images in different scale (a–b), corresponding elemental mapping Ca (c), P (d), O (e), and Pd (f) on the Pd<sup>0</sup>@nano-HAp catalyst surface obtained under *in-situ* conditions from the reduction of 4-NP.

decreases in the intensity of Bragg peaks in Pd<sup>0</sup>@nano-HAp can be explained by the presence of Pd<sup>0</sup> NPs on the surface, the charge distribution and changes in the electrostatic fields, and the interaction of the electrophilic surfaces with the frame oxygen atoms [91].

Images obtained from TEM analysis were used to determine the particle size/distribution of Pd nano clusters stabilized with hydroxyapatite. Fig. 2(a–c) depicts TEM images of Pd<sup>0</sup>@nano-HAp catalyst obtained under *in-situ* conditions from the reduction of 4-NP in different scale. It was observed in Fig. 2 that monodisperse Pd<sup>0</sup> NPs spread uniformly on the surface of the hydroxyapatite nanospheres. The mean diameter of Pd<sup>0</sup> NPs on the surface of hydroxyapatite nanospheres was found to be ~3 nm (Fig. 2 (d)) with a narrow particle size distribution using the NIH image program [92], which included the particle size analysis for >100 non-touching particles. The presence of Pd metal and other elements (calcium, phosphorus, oxygen and copper) derived from nano-HAp and TEM grid was confirmed in the analyzed region by EDX analysis of Pd<sup>0</sup>@nano-HAp catalyst (Fig. 2 (e)). Characteristic lattice fringes with crystal plane distances of 0.22 nm, indexable to the spacing of (111) planes in the *fcc* of Pd<sup>0</sup> NPs, were detected by the HR-TEM image of Pd<sup>0</sup>@nano-HAp (Fig. 2 (f)) [93].

SEM images obtained from the SEM analysis conducted to reveal the morphological structure of Pd<sup>0</sup>@nano-HAp catalyst and provided in Fig. 3(a–b) prove that Pd metal is successfully doped on the nanosphere structured hydroxyapatite solid support surface. In addition, elemental mapping images (Fig. 3(c–f)) obtained from a selected region provide information consistent TEM analysis of the elemental composition of the Pd<sup>0</sup>@nano-HAp catalyst and the mass densities of the said elements.

As shown in Fig. 4(a–b), to reveal the oxidation state and chemical structure of the elements in the Pd<sup>0</sup>@nano-HAp catalyst, XPS

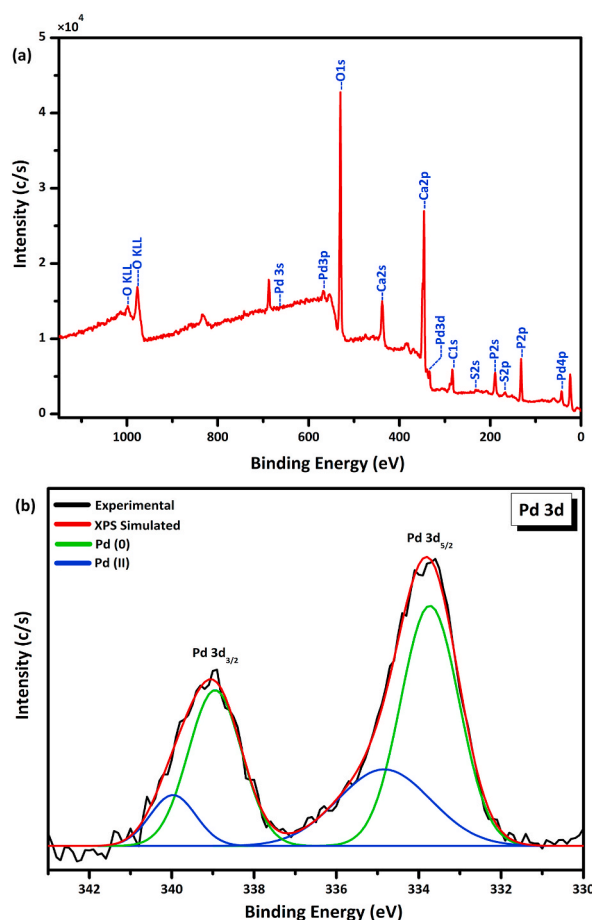


**Fig. 4.** Survey scan (a), and Pd 3 d core level (b) XPS spectra of Pd<sup>0</sup>@nano-HAp catalyst obtained under *in-situ* conditions from the reduction of 4-NP.

analysis was performed. The presence of Ca, P, O and Pd from the *nano*-HAp support and the Pd<sup>0</sup>@*nano*-HAp catalyst is shown in Fig. 4 (a). The high-resolution Pd 3 d core level XPS spectrum of Pd<sup>0</sup>@*nano*-HAp catalyst is seen in Fig. 4 (b) which contains two distinctive peaks for Pd 3d<sub>5/2</sub>, and 3d<sub>3/2</sub> at around 333.8 and 339.1 eV, corresponding to the Pd (0) 3 d (metallic). When Fig. 4 (b) is examined, it is seen that the Pd in the structure of the prepared Pd<sup>0</sup>@*nano*-HAp catalyst is mostly in metallic form [94,95].

The calculated BET surface area using BET equation following the BJH (Barrett–Joyner–Halanda) method was found to be as 21.9 m<sup>2</sup>/g for *nano*-HAp and 27.3 m<sup>2</sup>/g for Pd<sup>0</sup>@*nano*-HAp catalyst. Both catalysts' N<sub>2</sub> adsorption-desorption isotherms are consistent with the presence of mesoporous materials, as they conform to the IUPAC classification of type II and H3 hysteresis loops (Fig. 5) [96,97]. Total pore volume of Pd<sup>0</sup>@*nano*-HAp at p/p<sup>0</sup> = 0.98 is 0.17 cm<sup>3</sup> g<sup>-1</sup>. The results showed that incorporation of Pd<sup>0</sup> NPS onto the *nano*-HAp enhanced surface area is the beneficial for the development of a highly efficient catalyst.

### 3.2. The catalytic efficiency of Pd<sup>0</sup>@*nano*-HAp catalyst in the NPs reduction

The catalytic reduction of NPs in the presence of Pd<sup>0</sup>@*nano*-HAp catalyst was chosen as a model test reaction to view the catalytic activity of Pd<sup>0</sup>@*nano*-HAp catalyst. The kinetic parameters were determined by tracking the peaks where each substrate showed the strongest absorption bands (414 nm for 2-NP, 399 nm for 4-NP, 360 nm for 2,4-DNP and 391 nm for 2,4,6-TNP). By the catalyst-free self-hydrolysis of NaBH<sub>4</sub> (2), the conversion of nitrophenols to corresponding aminophenols in equivalent amounts was found to be very slow and to take 64 min for 2,4,6-TNP, 215 min for 2,4-DNP, 230 min for 4-NP and 240 min for 2-NP (Fig. S1).



However, even very low concentrations of Pd<sup>2+</sup>@*nano*-HAp precatalyst (Pd = 0.58 μmol) catalyze the reduction of nitrophenols to aminophenols at 298 K (Scheme 2), allowing rapid conversion (Fig. 5).

With the addition of NaBH<sub>4</sub> solution, it was observed that the absorption maxima of 2-NP, 4-NP, 2,4-DNP and 2,4,6-TNP at 414, 399, 360 and 391 nm changed to 282, 298, 438 and 304 nm, respectively. One of the most important reasons for these changes in the

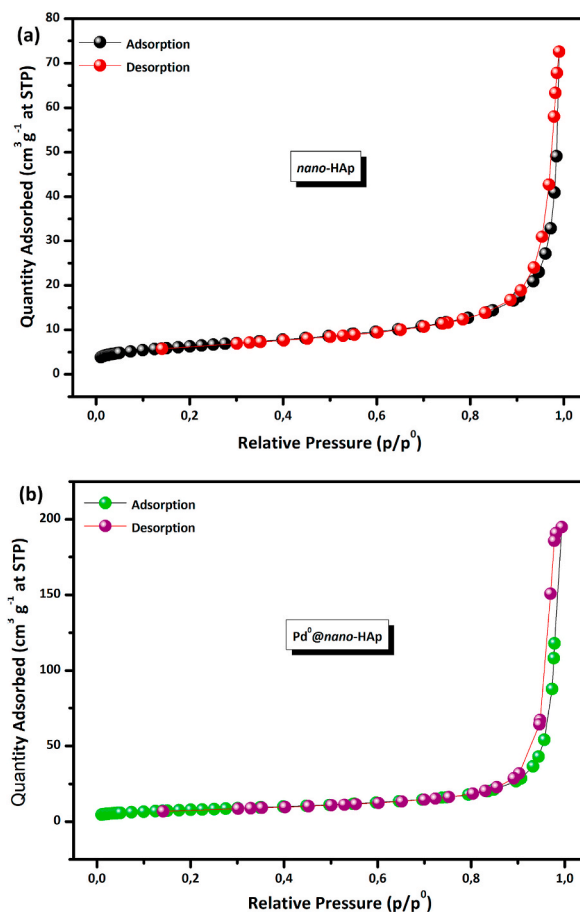
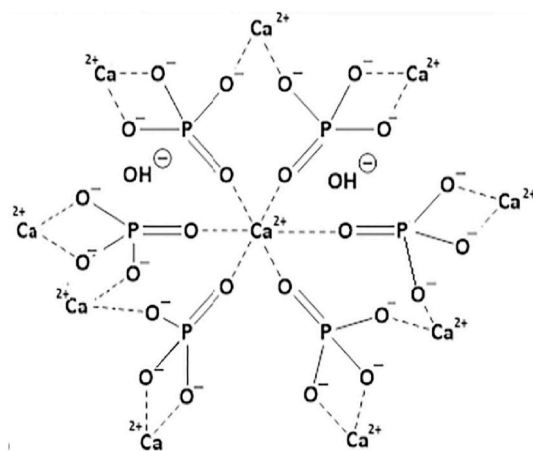
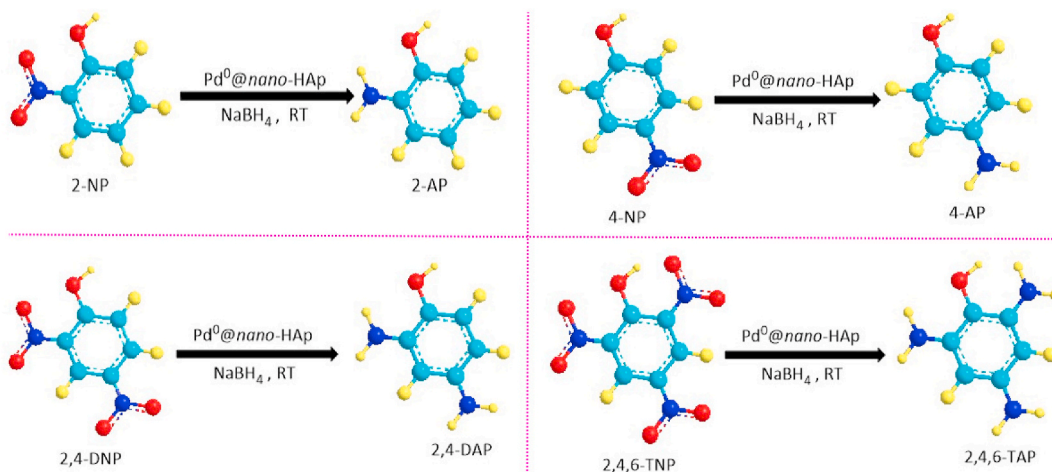


Fig. 5.  $N_2$  Adsorption-desorption isotherms of the *nano*-HAp (a) and  $Pd^0@nano$ -HAp catalyst (b).



Scheme 1. Molecular structure of HAP [98].

characteristic peaks is the structural changes that occur during the transformation of phenolate anions formed in the reaction medium into targeted products, while another reason is the significant decrease in both the intensity and ratio of the absorptive peaks in the presence of  $Pd^0@nano$ -HAp catalyst [72]. (Fig. 6(a–d)). Fig. 6(a–d) revealed that (i) the total conversion of nitrophenols happened within 0.5, 0.67, 4.5 and 0.67 min for the reduction of 2-NP, 4-NP, 2,4-DNP and 2,4,6-TNP to relevant aminophenols, respectively (ii) the initial rate of  $Pd^0@nano$ -HAp catalyzed reduction of nitrophenols at 298 K and  $Pd^0@nano$ -HAp catalyst concentration (0.58  $\mu$ mol)



**Scheme 2.** The reduction of the NP derivatives in the presence  $\text{Pd}^0@nano\text{-HAp}$  catalyst (cyan, blue, red, and yellow balls represent the elements of C, N, O, and H, respectively).

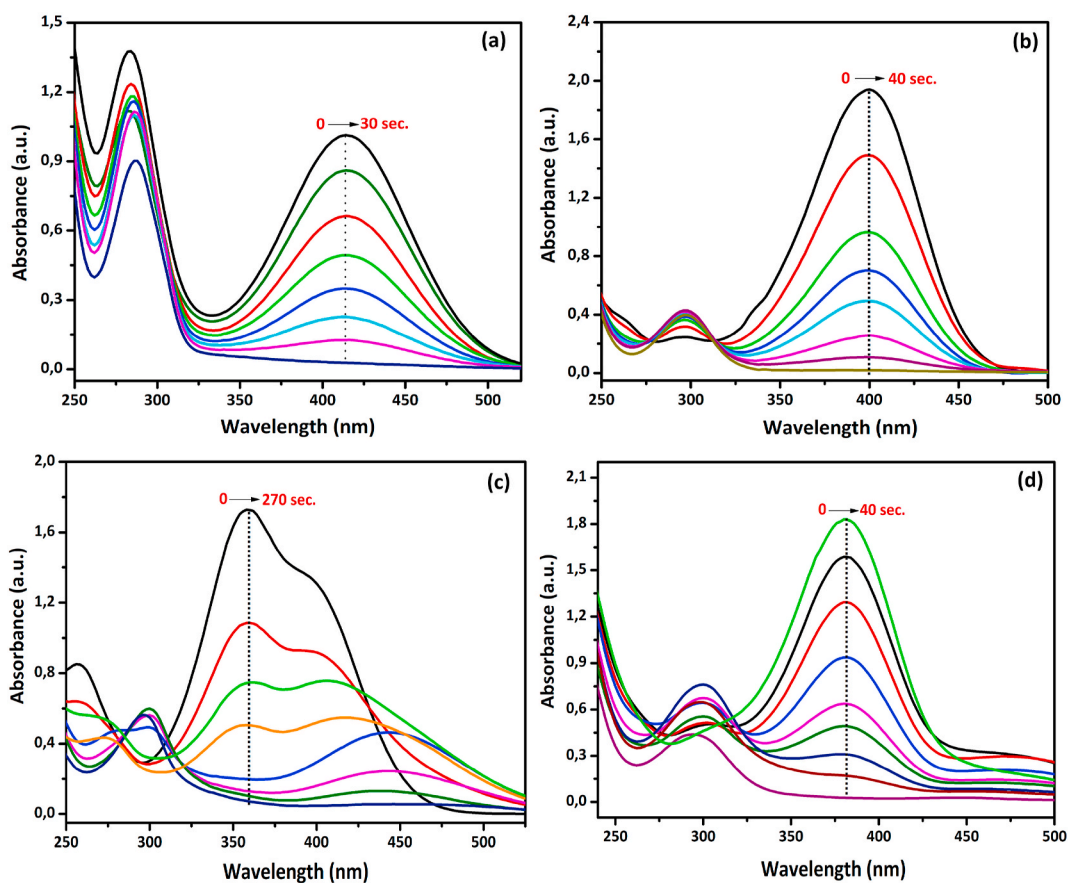


**Fig. 6.** UV-Vis spectra for the  $\text{Pd}^0@nano\text{-HAp}$  (0.58  $\mu\text{mol}$  Pd) catalyzed reduction of (a) 2-NP, (b) 4-NP, (c) 2,4-DNP, (d) 2,4,6-TNP in the aqueous  $\text{NaBH}_4$  (0.2 mmol) solution at room temperature under air.

followed the order of  $4\text{-NP} > 2\text{-NP} > 2,4,6\text{-TNP} > 2,4\text{-DNP}$ . The catalytic activity of the  $\text{Pd}^0@nano\text{-HAp}$  catalyst was tested in the reduction of nitrophenol derivatives in an aqueous medium in the presence of  $\text{NaBH}_4$  and the superb activity of  $\text{Pd}^0@nano\text{-HAp}$  catalyst has been detected against 2-NP, 4-NP, 2,4-DNP and 2,4,6-TNP derivatives with 70.6, 82.4, 27.6 and 41.4  $\text{min}^{-1}$  initial TOF values, respectively. It has been determined that these  $\text{TOF}_{\text{initial}}$  values recorded at room temperature are much higher than many

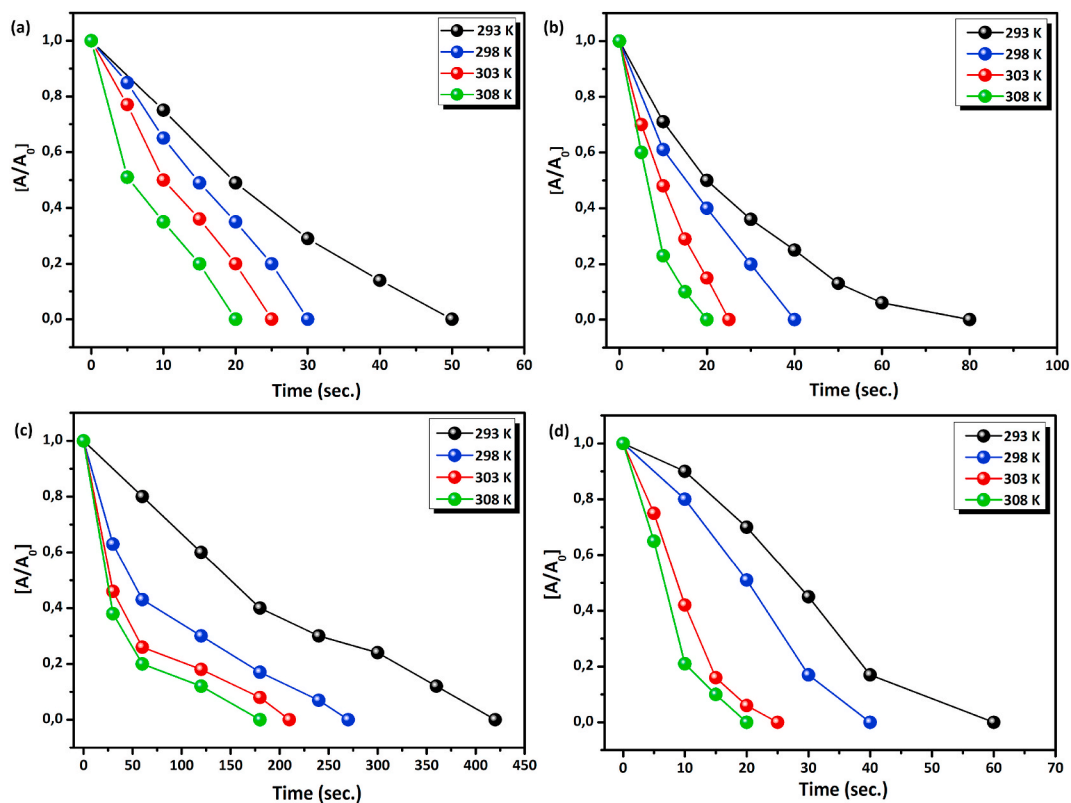


**Fig. 7.** The remaining fraction of nitrophenols versus time graph for Pd<sup>0</sup>@nano-HAp (0.58 μmol Pd) catalyzed the reduction of (a) 2-NP (b) 4-NP (c) 2,4-DNP and (d) 2,4,6-TNP in the aqueous NaBH<sub>4</sub> (0.2 mmol) solution at different temperatures in the range of 293–308 K.

existing studies in the literature. The remarkable activity of Pd<sup>0</sup>@nano-HAp catalyst can be attributed to (i) small sized and high dispersion of Pd<sup>0</sup> NPs on the support material surface and (ii) strong metal-support relation and synergy effect between nano-HAp and guest Pd<sup>0</sup> NPs.

### 3.3. Kinetic parameters for Pd<sup>0</sup>@nano-HAp catalyzed the reduction of nitrophenols

The influence of temperature on the reduction of nitrophenols was determined and the activation parameters were calculated with the help of repeated experiments in the temperature range of 298–318 K increases for every 5 K and catalyzed by Pd<sup>0</sup>@nano-HAp (Fig. 7). Observed rate constants ( $k_{obs}$ ) were calculated separately for each temperature in the graphs drawn for  $[A]/[A_0]$  versus time (Fig. 7(a–d)). Activation energy ( $E_a$ ), enthalpy ( $\Delta H^\ddagger$ ) and entropy ( $\Delta S^\ddagger$ ) parameters were calculated from the slopes of the Arrhenius and Eyring-Polanyi plots (Fig. 8(a–b)) drawn using  $k_{obs}$  values and the Arrhenius and Eyring-Polanyi equations. When examining the activation parameters during the conversion of nitrophenols to aminophenols (in Table 1), assuming that the calculated apparent activation parameters using the kinetic data are related the most important activation step that directs the reaction mechanism in the conversion of nitrophenols to aminophenols, one can argue that the positive magnitude of the apparent activation enthalpy and large negative value of the apparent activation entropy imply the presence of an associative reaction step revealing a transition state [99, 100].

### 3.4. Catalytic durability of Pd<sup>0</sup>@nano-HAp in the NPs reduction

In the experiments carried out to determine the catalytic resistance and stability of the prepared Pd<sup>0</sup>@nano-HAp catalyst, the isolated catalyst was dried and purified and reused after each conversion was completed. Also, the need for more precise replacement of the catalytic reaction followed by UV–vis spectroscopy from the solvent-substrate-product solution to the second catalytic cycle occurred. This situation can be explained as another reason why we prefer reusability experiments in terms of recyclability in order to determine the durability of the catalyst used. The studied catalytic system provided ~69–93 % of initial activity in the reduction of NPs, and this was confirmed by the results of reusability experiments. The reusability performance, which is accepted as one of the most basic criteria determining the performance and usability of the nanoparticles used as a catalyst, was also tested for the Pd<sup>0</sup>@nano-HAp catalyst in the reduction of NP derivatives at 298 K. For each substrate intended to be reduced, the Pd<sup>0</sup>@nano-HAp catalyst was isolated by filtration after the catalytic reaction was completely finished. After the obtained catalyst was washed with ethanol-water

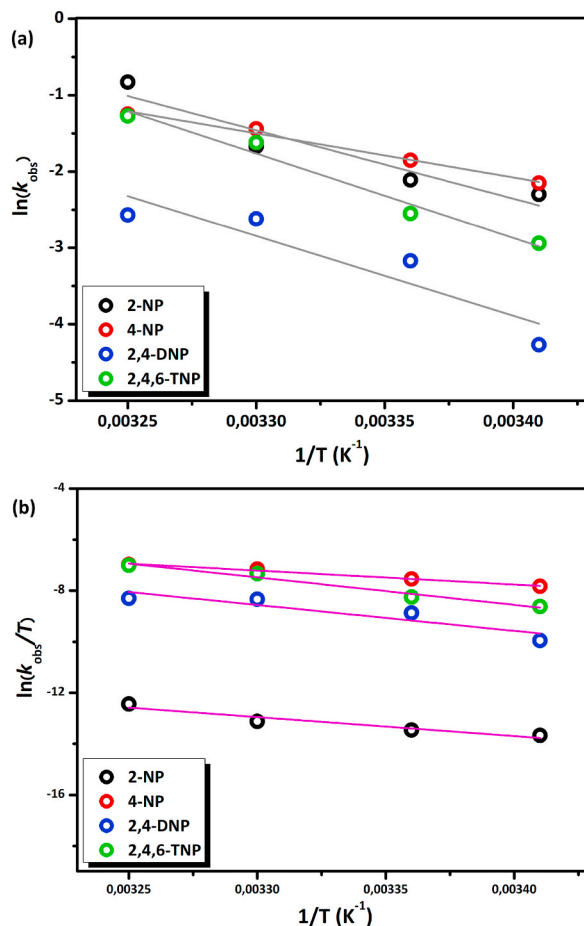


**Fig. 8.** (A) Arrhenius (gray line) and (b) Eyring-Polanyi (magenta line) plots for Pd<sup>0</sup>@nano-HAp (0.58 μmol Pd) catalyzed the reduction of nitrophenols in the aqueous NaBH<sub>4</sub> (0.2 mmol) solution.

**Table 1**

Activation parameters for the Pd<sup>0</sup>@nano-HAp catalyzed the reduction of nitrophenols, in aqueous solution of NaBH<sub>4</sub>.

Substrate	$E_a$ (kJ × mol <sup>-1</sup> )	$\Delta H^\ddagger$ (kJ × mol <sup>-1</sup> )	$\Delta S^\ddagger$ (J × mol <sup>-1</sup> × K <sup>-1</sup> )
2-NP	74.9	61.8	-101.1
4-NP	48	45.4	-107.8
2,4-DNP	86.8	84.4	+9.8
2,4,6-TNP	91.9	89.5	+35.7

mixture, it was dried in vacuum at 353 K. With these processes, the Pd<sup>0</sup>@nano-HAp catalyst was made ready for reuse. By adding Pd<sup>0</sup>@nano-HAp catalyst and the same amount of substrate as used in the previous experiment to the reaction vessel and restarting the reaction under the same conditions, it was determined that the catalyst activity continued to a great extent (Fig. 9). The results obtained by interpreting the data obtained from the catalytic studies are illuminating that Pd<sup>0</sup>@nano-HAp catalyst retains 87.8, 68.5, 90.2 and 92.8 % of its initial activity even at 5th catalytic reuse (Fig. 9(a-d)) in the hydrogenation of 2-NP, 4-NP, 2,4-DNP and 2,4,6-TNP, respectively.

The highly acceptable reusability performance of the Pd<sup>0</sup>@nano-HAp catalyst against each substrate used in the reduction reaction is largely due to the high stability of the Pd<sup>0</sup> NPs, which inhibits bulk Pd formation. However, the small amount of activity loss observed at the end of the catalytic reuse experiments is largely due to the reduction in the number of active atoms on the surface. This reduction is due to partial aggregation resulting from the aggregation of Pd<sup>0</sup> NPs as shown in the labeled portions in Fig. 10 (a). In addition, the increase in particle size (from 3.02 nm to 3.74 nm) is also considered as another important reason for the loss of efficiency (Fig. 10 (b)). SEM analysis was also performed to reveal the morphological stability of the spent Pd<sup>0</sup>@nano-HAp catalyst. From the SEM and elemental mapping images shown in Fig. S2, it is understood that the Pd<sup>0</sup> NPs generally show homogeneous distribution and show high stability except for partial aggregation in some regions. It was confirmed by the XRD result that the crystal structure of the

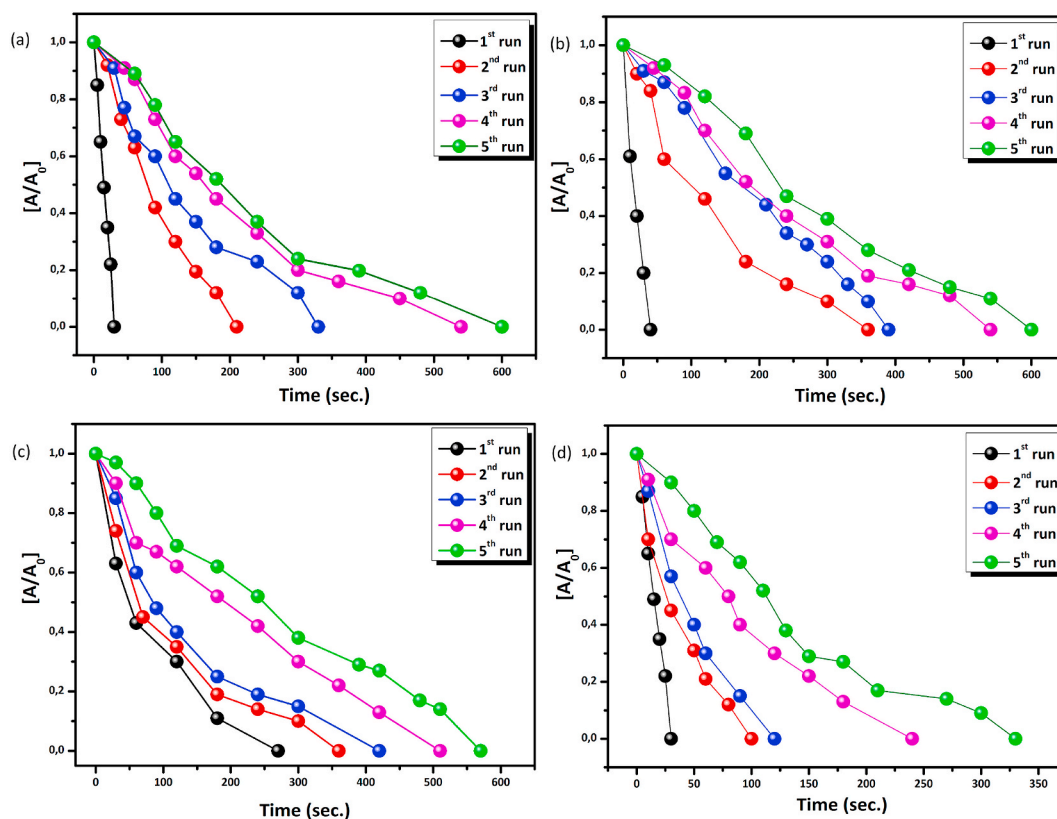


Fig. 9. The remaining fraction of nitrophenols versus time graph for the reusability performance of Pd<sup>0</sup>@nano-HAp in the catalytic reduction of (a) 2-NP, (b) 4-NP, (c) 2,4-DNP and (d) 2,4,6-TNP.

catalyst remained nearly unchanged with the reuse of Pd<sup>0</sup>@nano-HAp during the reduction of 4-NP (Fig. S3).

#### 4. Conclusions

The remarkable results in the synthesis, characterization of Pd<sup>0</sup> NPs supported over hydroxyapatite nanospheres (Pd<sup>0</sup>@nano-HAp) and tests in which they used as catalyst in the reduction of different nitrophenol derivatives in the presence of NaBH<sub>4</sub> as reducing agent can be listed as follows.

- (I) Pd<sup>0</sup>@nano-HAp catalyst was reproducibly synthesized by the ion-exchange of Pd<sup>2+</sup> onto hydroxyapatite nanospheres under *in-situ* conditions during the catalytic reduction of NP derivatives in aqueous media at 298 K,
- (II) It has been observed that monodisperse Pd<sup>0</sup> NPs are uniformly fixed on the nano-HAp surface in the Pd<sup>0</sup>@nano-HAp catalyst characterized by various techniques such as ICP-OES, *P*-XRD, XPS, TEM, SEM and BET,
- (III) In the reduction experiments of nitrophenols in aqueous solution of NaBH<sub>4</sub> at moderate conditions, it was determined that the Pd<sup>0</sup>@nano-HAp catalyst, whose both catalytic activity and stability were examined, is a highly active catalyst in the conversion of nitrophenols to their aminophenol analogs. The excellent catalytic activity of the Pd<sup>0</sup>@nano-HAp catalyst was supported by the 70.6, 82.4, 27.6 and 41.4 min<sup>-1</sup> TOF<sub>initial</sub> values found for 2-NP, 4-NP, 2,4-DNP and 2,4,6-TNP, respectively, which are among the highest of the catalytic systems tested in the reduction of nitrophenols,
- (IV) Additionally, the Pd<sup>0</sup>@nano-HAp catalyst exhibited outstanding resistance to sintering during catalytic operations, thereby maintaining its activity in the range of 68.5 %–92.8 % even after the 5th catalytic reuse.
- (V) The excellent stability, high activity and good reusability of the Pd<sup>0</sup>@nano-HAp catalyst make it a great candidate for this kind industrial and commercial applications.
- (VI) This study also presents a robust catalyst and clues of catalyst design for the selective catalytic reduction of other nitroaromatics to produce amines.

#### Data availability statement

Data will be made available on request.

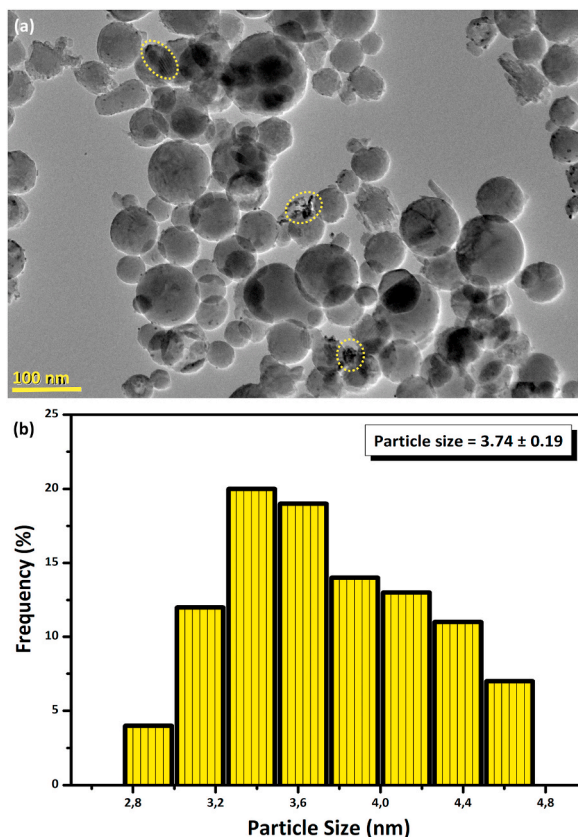


**Fig. 10.** TEM image taken in 100 nm scale (a) and corresponding particle size histogram (b) of Pd<sup>0</sup>@nano-HAp sample collected after the fifth reuse from the reduction of 4-NP.

#### CRediT authorship contribution statement

**Adem Rüzgar:** Conceptualization, Formal analysis, Investigation, Writing – original draft. **Yaşar Karataş:** Formal analysis, Investigation, Methodology. **Mehmet Gülcan:** Project administration, Supervision, Writing – review & editing.

#### Declaration of competing interest

The authors declare that they have no known competing financial interests or personal relationships that could have appeared to influence the work reported in this paper.

#### Acknowledgement

We are grateful to Van YYÜ BAP unit for their support (Project ID: FYD-2022-9983).

#### Appendix A. Supplementary data

Supplementary data to this article can be found online at <https://doi.org/10.1016/j.heliyon.2023.e21517>.

#### References

- [1] Z.M. El-Bahy, Preparation and characterization of Pt-promoted NiY and CoY catalysts employed for 4-nitrophenol reduction, *Appl. Catal., A* 468 (2013) 175–183.
- [2] Y. Zhang, Y. Kuwahara, K. Mori, H. Yamashita, Construction of hybrid MoS<sub>2</sub> phase coupled with SiC heterojunctions with promoted photocatalytic activity for 4-nitrophenol degradation, *Langmuir* 36 (2020) 1174–1182.
- [3] E. Akbarzadeh, M.R. Gholami, Pt–NiO–Al<sub>2</sub>O<sub>3</sub>/G derived from graphene-supported layered double hydroxide as efficient catalyst for *p*-nitrophenol reduction, *Res. Chem. Intermed.* 43 (2017) 5829–5839.

- [4] K. Sahu, B. Satpati, R. Singhal, S. Mohapatra, Enhanced catalytic activity of CuO/Cu<sub>2</sub>O hybrid nanowires for reduction of 4-nitrophenol in water, *J. Phys. Chem. Solid.* 136 (2020), 109143.
- [5] K. Shamsa, P.S. MaryRajitha, S. Vinoth, C. Murugan, P. Rameshkumar, A. Pandikumar, In situ formed zinc oxide/graphitic carbon nitride nanohybrid for the electrochemical determination of 4-nitrophenol, *Microchim. Acta* 552 (2020) 187.
- [6] H.G. Soğukömerogulları, Y. Karataş, M. Çelebi, M. Gülcan, M. Sönmez, M. Zahmakiran, Palladium nanoparticles decorated on amine functionalized graphene nanosheets as excellent nanocatalyst for the hydrogenation of nitrophenols to aminophenol counterparts, *J. Hazard Mater.* 369 (2019) 96–107.
- [7] O.A. Osin, T. Yu, X. Cai, Y. Jiang, G. Peng, X. Cheng, R. Li, Y.S. Qin, S. Lin, Photocatalytic degradation of 4-nitrophenol by C, N-TiO<sub>2</sub>: degradation efficiency vs. embryonic toxicity of the resulting compounds, *Front. Chem.* 6 (2018) 192.
- [8] M. Sudha, G. Renu, G. Sangeeta, Mineralization and degradation of 4-nitrophenol using homogeneous Fenton oxidation process, *Environ. Eng. Res.* 26 (2021) 3.
- [9] Y.-T. Woo, D.Y. Lai, *Aromatic Amino and Nitro-Amino Compounds and Their Halogenated Derivatives*, Patty's Toxicology Wiley, New York, 2001, pp. 1–96.
- [10] H. Wu, H. Li, Z. Fang, Hydrothermal amination of biomass to nitrogenous chemicals, *Green Chem.* 23 (2021) 6675–6697.
- [11] H. Li, H. Guo, Y. Su, Y. Hiraga, Z. Fang, E.J.M. Hensen, M. Watanabe, R.L. Smith, N-formyl-stabilizing quasi-catalytic species afford rapid and selective solvent-free amination of biomass-derived feedstocks, *Nat. Commun.* 10 (2019) 699.
- [12] X.F. Zhang, X.Y. Zhu, J.J. Feng, A.J. Wang, Solvothermal synthesis of N-doped graphene supported PtCo nanodendrites with highly catalytic activity for 4-nitrophenol reduction, *Appl. Surf. Sci.* 428 (2018) 798–808.
- [13] R. Grzeschik, D. Schäfer, T. Holtum, S. Küpper, A. Hoffmann, S. Schlücker, On the overlooked critical role of the pH value on the kinetics of the 4-nitrophenol NaBH<sub>4</sub> reduction catalyzed by noble-metal nanoparticles (Pt, Pd, and Au), *J. Phys. Chem. C* 124 (2020) 2939–2944.
- [14] J.-H. Noh, R. Meijboom, Synthesis and catalytic evaluation of dendrimer-templated and reverse microemulsion Pd and Pt nanoparticles in the reduction of 4-nitrophenol: the effect of size and synthetic methodologies, *Appl. Catal.* 497 (2015) 107–120.
- [15] E. Akbarzadeh, H.Z. Soheili, M.R. Gholami, Novel Cu<sub>2</sub>O/Cu-MOF/rGO is reported as highly efficient catalyst for reduction of 4-nitrophenol, *Mater. Chem. Phys.* 237 (2019), 121846.
- [16] K. Sahu, J. Singh, S. Mohapatra, Catalytic reduction of 4-nitrophenol and photocatalytic degradation of organic pollutants in water by copper oxide nanosheets, *Opt. Mater.* 93 (2019) 58–69.
- [17] Z. Wang, L. Li, M. Liu, T. Miao, X. Ye, S. Meng, S. Chen, X. Fu, A new phosphidation route for the synthesis of NiPx and their cocatalytic performances for photocatalytic hydrogen evolution over g-C<sub>3</sub>N<sub>4</sub>, *J. Energy Chem.* 48 (2020) 241–249.
- [18] N. Wang, F. Wang, F. Pan, S. Yu, D. Pan, Highly efficient silver catalyst supported by a spherical covalent organic framework for the continuous reduction of 4-nitrophenol, *ACS Appl. Mater. Interfaces* 13 (2021) 3209–3220.
- [19] G. Ravi, M. Sarasija, D. Ayodhya, L.S. Kumari, D. Ashok, Facile synthesis, characterization and enhanced catalytic reduction of 4-nitrophenol using NaBH<sub>4</sub> by undoped and Sm<sup>3+</sup>, Gd<sup>3+</sup>, Hf<sup>3+</sup> Doped La<sub>2</sub>O<sub>3</sub> nanoparticles, *Nano Converg* 6 (2019) 12.
- [20] C. Chu, S. Rao, Z. Ma, H. Han, Copper and cobalt nanoparticles doped nitrogen-containing carbon frameworks derived from CuO-encapsulated ZIF-67 as high-efficiency catalyst for hydrogenation of 4-nitrophenol, *Appl. Catal. B Environ.* 256 (2019), 117792.
- [21] P. Deka, R.C. Deka, P. Bharali, In situ generated copper nanoparticle catalyzed reduction of 4-nitrophenol, *New J. Chem.* 38 (2014) 1789–1793.
- [22] X. Sun, P. He, Z. Gao, Y. Liao, S. Weng, Z. Zhao, H. Song, Z. Zhao, Multi-crystalline N-doped Cu/Cu<sub>x</sub>O/C foam catalyst derived from alkaline N-coordinated HKUST-1/CMC for enhanced 4-nitrophenol reduction, *J. Colloid Interface Sci.* 553 (2019) 1–13.
- [23] Y. Tian, Y.Y. Cao, F. Pang, G.Q. Chen, X. Zhang, Ag nanoparticles supported on N-doped graphene hybrids for catalytic reduction of 4-nitrophenol, *RSC Adv.* 4 (2014) 43204–43211.
- [24] Z. Hasan, D.W. Cho, C.M. Chon, K. Yoon, H. Song, Reduction of *p*-nitrophenol by magnetic Co-carbon composites derived from metal organic frameworks, *Chem. Eng. J.* 298 (2016) 183–190.
- [25] A.A. Kassem, H.N. Abdelhamid, D.M. Fouad, S.A. Ibrahim, Catalytic reduction of 4-nitrophenol using copper terephthalate frameworks and CuO@C composite, *J. Environ. Chem. Eng.* 9 (2021), 104401.
- [26] J. Li, L. Zhang, X. Liu, N. Shang, S. Gao, C. Feng, C. Wang, Z. Wang, Pd nanoparticles supported on a covalent triazinebased framework material: an efficient and highly chemoselective catalyst for the reduction of nitroarenes, *New J. Chem.* 42 (2018) 9684–9689.
- [27] Y. Zhao, B. Cao, Z. Lin, X. Su, Synthesis of CoFe<sub>2</sub>O<sub>4</sub>/C nano-catalyst with excellent performance by molten salt method and its application in 4-nitrophenol reduction, *Environ. Pollut.* 254 (2019), 112961.
- [28] Y. Zhou, Y. Zhu, X. Yang, J. Huang, W. Chen, X. Lv, C. Li, C. Li, Au decorated Fe<sub>3</sub>O<sub>4</sub>@TiO<sub>2</sub> magnetic composites with visible light-assisted enhanced catalytic reduction of 4-nitrophenol, *RSC Adv.* 5 (2015) 50454–50461.
- [29] R. Das, V.S. Sypu, H.K. Paumo, M. Bhaumik, V. Maharaj, A. Maity, Silver decorated magnetic nanocomposite (Fe<sub>3</sub>O<sub>4</sub>@PPy-MAA/Ag) as highly active catalyst towards reduction of 4-nitrophenol and toxic organic dyes, *Appl. Catal. B Environ.* 244 (2019) 546–558.
- [30] S. Jiang, H. Ni, P. Li, J. Wang, H. Ren, Metal/N-doped carbon (Metal = Ag, Cu, Ni) nanocatalysts for selective hydrogenation of 4-nitrophenol, *Catal. Commun.* 151 (151) (2021), 106280.
- [31] S. Kapoor, A. Sheoran, M. Riyaz, J. Agarwal, N. Goel, S. Singhal, Enhanced catalytic performance of Cu/Cu<sub>2</sub>O nanoparticles via introduction of graphene as support for reduction of nitrophenols and ring opening of epoxides with amines established by experimental and theoretical investigations, *J. Catal.* 381 (2020) 329–346.
- [32] A.T.E. Villian, S.R. Choe, K. Giribabu, S.-C. Jang, C. Roh, Y.S. Huh, Y.-K. Han, Pd nanospheres decorated reduced graphene oxide with multi-functions: highly efficient catalytic reduction and ultrasensitive sensing of hazardous 4-nitrophenol pollutant, *J. Hazard Mater.* 333 (2017) 54–62.
- [33] N.I. Ikhsan, P. Rameshkumar, N.M. Huang, Controlled synthesis of reduced graphene oxide supported silver nanoparticles for selective and sensitive electrochemical detection of 4-nitrophenol, *Electrochim. Acta* 192 (2016) 392–399.
- [34] Y. Cheng, A sensor for detection of 4-nitrophenol based on a glassy carbon electrode modified with a reduced graphene oxide/Fe<sub>3</sub>O<sub>4</sub> nanoparticle composite, *Int. J. Electrochem. Sci.* 8 (2017) 7754–7764.
- [35] M.I. Din, R. Khalid, Z. Hussain, T. Hussain, A. Mujahid, J. Najeeb, F. Izhar, Nanocatalytic assemblies for catalytic reduction of nitrophenols: a critical review, *Crit. Rev. Anal. Chem.* 50 (2020) 322–338.
- [36] X.-K. Kong, Z.-Y. Sun, M. Chen, C.-K. Chen, Q.-W. Chen, Metal-free catalytic reduction of 4-nitrophenol to 4-aminophenol by N-doped graphene, *Energy Environ. Sci.* 6 (11) (2013) 3260–3266.
- [37] B. Li, Z. Xu, A nonmetal catalyst for molecular hydrogen activation with comparable catalytic hydrogenation capability to noble metal catalyst, *J. Am. Chem. Soc.* 131 (45) (2009) 16380–16382.
- [38] W. Xiong, Z. Wang, S. He, F. Hao, Y. Yang, Y. Lv, W. Zhang, P. Liu, H.a. Luo, Nitrogen-doped carbon nanotubes as a highly active metal-free catalyst for nitrobenzene hydrogenation, *Appl. Catal. B Environ.* 260 (2020), 118105.
- [39] S. Yu, H. Pang, S. Huang, H. Tang, S. Wang, M. Qiu, Z. Chen, H. Yang, G. Song, D. Fu, B. Hu, X. Wang, Recent advances in metal-organic framework membranes for water treatment: a review, *Sci. Total Environ.* 800 (2021), 149662.
- [40] G. Chen, R. Shan, J. Shi, C. Liu, B. Yan, Biodiesel production from palm oil using active and stable K doped hydroxyapatite catalysts, *Energy Convers. Manag.* 98 (2015) 463–469.
- [41] J. Kamieniak, P.J. Kelly, C.E. Banks, A.M. Doyle, Methane emission management in a dual-fuel engine exhaust using Pd and Ni hydroxyapatite catalysts, *Fuel* 208 (2017) 314–320.
- [42] Z.C. Xiong, Z.Y. Yang, Y.J. Zhu, F.F. Chen, R.L. Yang, D.D. Qin, Ultralong hydroxyapatite nanowire-based layered catalytic paper for highly efficient continuous flow reactions, *J. Mater. Chem. A* 6 (2018) 5762–5773.
- [43] A. Safavi, S. Momeni, Highly efficient degradation of azo dyes by palladium/hydroxyapatite/Fe<sub>3</sub>O<sub>4</sub> nanocatalyst, *J. Hazard Mater.* 201–202 (2012) 125–131.
- [44] M. He, H. Shi, X.Y. Zhao, Y. Yu, B. Qu, Immobilization of Pb and Cd in contaminated soil using nanocrystallite hydroxyapatite, *Procedia Environ. Sci.* 18 (2013) 657–665.

- [45] L. Ma'mani, M. Sheykhani, A. Heydari, M. Faraji, Y. Yamini, Sulfonic acid supported on hydroxyapatite-encapsulated- $\gamma$ -Fe<sub>2</sub>O<sub>3</sub> nanocrystallites as a magnetically Brønsted acid for N-formylation of amines, *Appl. Catal.* 377 (2010) 64–69.
- [46] J. Deng, L.P. Mo, F.Y. Zhao, L.L. Hou, L. Yang, Z.H. Zhang, Sulfonic acid supported on hydroxyapatite-encapsulated- $\gamma$ -Fe<sub>2</sub>O<sub>3</sub> nanocrystallites as a magnetically separable catalyst for one-pot reductive amination of carbonyl compounds, *Green Chem.* 13 (2011) 2576–2584.
- [47] S. Bahadorikhalili, H. Arshadi, Z. Afrouzandeh, L. Ma'mani, Ultrasonic promoted synthesis of Ag nanoparticle decorated thiourea-functionalized magnetic hydroxyapatite: a robust inorganic-organic hybrid nanocatalyst for oxidation and reduction reactions, *New J. Chem.* 44 (2020) 8840–8848.
- [48] C.S. Ciobanu, S.L. Iconaru, M.C. Chifriuc, A. Costescu, P.L. Coustumer, D. Predoi, Synthesis and antimicrobial activity of silver-doped hydroxyapatite nanoparticles, *BioMed Res. Int.* 2013 (2013), 916218.
- [49] A. Grandjean-Laquerriere, P. Laquerriere, E. Jallot, J.-M. Nedelec, M. Guenounou, D. Laurent-Maquin, T.M. Phillips, Influence of the zinc concentration of sol-gel derived zinc substituted hydroxyapatite on cytokine production by human monocytes in vitro, *Biomaterials* 27 (2006) 3195–3200.
- [50] A.C. Tas, Synthesis of biomimetic Ca-hydroxyapatite powders at 37 degrees C in synthetic body fluids, *Biomaterials* 21 (2000) 1429–1438.
- [51] X. Guo, H. Yan, S. Zhao, Z. Li, Effect of calcining temperature on particle size of hydroxyapatite synthesized by solid-state reaction at room temperature, *Adv. Powder Technol.* 4 (6) (2013) 1034–1038.
- [52] I. Kimura, Synthesis of hydroxyapatite by interfacial reaction in a multiple emulsion, *Res. Lett. Mater. Sci.* (2007), 71284.
- [53] M. Shikhanzadeh, Direct formation of nanophase hydroxyapatite on cathodically polarized electrodes, *J. Mater. Sci. Mater. Med.* 9 (1998) 67–72.
- [54] A. Jilavenkatesa, R.A. Condrate SR, Sol-gel processing of hydroxyapatite, *J. Mater. Sci.* 33 (1998) 4111–4119.
- [55] T.A. Kuriakosea, S.N. Kalkura, M. Palanichami, D. Arivuoli, K. Dierks, G. Bocelli, C. Betzel, Synthesis of stoichiometric nano crystalline hydroxyapatite by ethanol-based sol-gel technique at low temperature, *J. Cryst. Growth* 263 (2004) 517–523.
- [56] K. Yamashita, T. Arashi, K. Kitagaki, S. Yamada, T. Umegaki, Preparation of apatite thin films through rf sputtering from calcium phosphate glasses, *J. Am. Ceram. Soc.* 77 (9) (1994) 2401–2407.
- [57] O.V. Sinitayna, A.G. Veresov, E.S. Kovaleva, Y.V. Kolen'ko, Synthesis of hydroxyapatite by hydrolysis of  $\alpha$ -Ca<sub>3</sub>(PO<sub>4</sub>)<sub>2</sub>, *Russ. Chem. Bull.* 54 (2005) 79–86.
- [58] K. Mori, T. Hara, T. Mizugaki, K. Ebitani, K. Kaneda, Hydroxyapatite-supported palladium nanoclusters: a highly active heterogeneous catalyst for selective oxidation of alcohols by use of molecular oxygen, *J. Am. Chem. Soc.* 126 (2004) 10657–10666.
- [59] C.M. Ho, W.Y. Yu, C.M. Che, Ruthenium nanoparticles supported on hydroxyapatite as an efficient and recyclable catalyst for cis-dihydroxylation and oxidative cleavage of alkenes, *Angew. Chem. Int. Ed.* 43 (2004) 3303–3307.
- [60] M. Zahmakiran, Y. Tonbul, S. Özkar, Ruthenium (0) nanoclusters supported on hydroxyapatite: highly active, reusable and green catalyst in the hydrogenation of aromatics under mild conditions with an unprecedented catalytic lifetime, *Chem. Commun.* 46 (2010) 4788–4790.
- [61] T. Mitsudome, S. Arita, K. Mori, T. Mizugaki, K. Jitsukawa, K. Kaneda, Supported silver-nanoparticle-catalyzed highly efficient aqueous oxidation of phenylsilanes to silanols, *Angew. Chem. Int. Ed.* 47 (2008) 7938–7940.
- [62] T.K. Das, S. Ganguly, P. Bhawal, S. Mondal, N.C. Das, A facile green synthesis of silver nanoparticle-decorated hydroxyapatite for efficient catalytic activity towards 4-nitrophenol reduction, *Res. Chem. Intermed.* 44 (2018) 1189–1208.
- [63] T.T.T.L. Hoang, N. Insin, N. Sukpirom, Catalytic activity of silver nanoparticles anchored on layered double hydroxides and hydroxyapatite, *Inorg. Chem. Commun.* 121 (2020), 108199.
- [64] Y. Liu, H. Tsunoyama, T. Akita, T. Tsukuda, Efficient and selective epoxidation of styrene with TBHP catalyzed by Au<sub>25</sub> clusters on hydroxyapatite, *Chem. Commun.* 46 (2010) 550–552.
- [65] K.C. Das, S.S. Dhar, Fast catalytic reduction of p-nitrophenol by Cu/HAP/ZnFe<sub>2</sub>O<sub>4</sub> nanocomposite, *Mater. Sci. Eng. B* 263 (2021), 114841.
- [66] Z. Yaakob, L. Hakim, M.N.S. Kumar, M. Ismail, W.R.W. Daud, Hydroxyapatite supported Nickel catalyst for hydrogen production, *Am. J. Sci. Ind. Res.* 1 (2010) 122–126.
- [67] A. Indra, C.S. Gopinath, S. Bhaduri, G.K. Lahiri, Hydroxyapatite supported palladium catalysts for Suzuki-Miyaura cross-coupling reaction in aqueous medium, *Catal. Sci. Technol.* 3 (6) (2013) 1625–1633.
- [68] C. Li, G. Xu, X. Liu, Y. Zhang, Y. Fu, Hydrogenation of biomass-derived furfural to tetrahydrofurfuryl alcohol over hydroxyapatite-supported Pd catalyst under mild conditions, *Ind. Eng. Chem. Res.* 56 (31) (2017) 8843–8849.
- [69] O.S. Chambyal, S. Paul, T. Shamim, M. Gupta, R. Gupta, A. Loupy, HAP-Pd(0): a highly efficient recyclable heterogeneous catalyst for the selective reduction of carbon-carbon double bond in alpha, beta-unsaturated ketones, *Synth. Commun.* 43 (5) (2013) 656–667.
- [70] M. Rakap, S. Özkar, Hydroxyapatite-supported cobalt (0) nanoclusters as efficient and cost-effective catalyst for hydrogen generation from the hydrolysis of both sodium borohydride and ammonia-borane, *Catal. Today* 183 (2012) 17–25.
- [71] N. Akhlaghi, G. Najafpour-Darzi, Manganese ferrite (MnFe<sub>2</sub>O<sub>4</sub>) nanoparticles: from synthesis to application-A review, *J. Ind. Eng. Chem.* 103 (2021) 292–304.
- [72] K. Karakas, A. Celebioglu, M. Celebi, T. Uyar, M. Zahmakiran, Nickel nanoparticles decorated on electrospun polycaprolactone/chitosan nanofibers as flexible, highly active and reusable nanocatalyst in the reduction of nitrophenols under mild conditions, *Appl. Catal. B Environ.* 203 (2017) 549–562.
- [73] Y. Fu, P. Xu, D. Huang, G. Zeng, C. Lai, L. Qin, B. Li, J. He, H. Yi, M. Cheng, C. Zhang, Au nanoparticles decorated on activated coke via a facile preparation for efficient catalytic reduction of nitrophenols and azo dyes, *Appl. Surf. Sci.* 473 (2019) 578–588.
- [74] B. Baruah, G.J. Gabriel, M.J. Akbashev, M.E. Booher, Facile synthesis of silver nanoparticles stabilized by cationic polynorbornenes and their catalytic activity in 4-nitrophenol reduction, *Langmuir* 29 (2013) 4225–4234.
- [75] X. Duan, J. Liu, J. Hao, L. Wu, B. He, Y. Qiu, J. Zhang, Z. He, J. Xi, S. Wang, Magnetically recyclable nanocatalyst with synergetic catalytic effect and its application for 4-nitrophenol reduction and Suzuki coupling reactions, *Carbon* 130 (2018) 806–813.
- [76] J. Xi, H. Sun, D. Wang, Z. Zhang, X. Duan, J. Xiao, F. Xiao, L. Liu, S. Wang, Confined-interface-directed synthesis of palladium single-atom catalysts on graphene/amorphous carbon, *Appl. Catal. B Environ.* 225 (2018) 291–297.
- [77] J. Liu, J. Hao, C. Hu, B. He, J. Xi, J. Xiao, S. Wang, Z. Bai, Palladium nanoparticles anchored on amine-functionalized silica nanotubes as a highly effective catalyst, *J. Phys. Chem. C* 122 (2018) 2696–2703.
- [78] X. Duan, M. Xiao, S. Liang, Z. Zhang, Y. Zeng, J. Xi, S. Wang, Ultrafine palladium nanoparticles supported on nitrogen-doped carbon microtubes as a high-performance organocatalyst, *Carbon* 119 (2017) 326–331.
- [79] J. Xi, J. Xiao, F. Xiao, Y. Jin, Y. Dong, F. Jing, S. Wang, Mussel-inspired functionalization of cotton for nanocatalyst support and its application in a fixed-bed system with high performance, *Sci. Rep.* 6 (2016) 21904–21911.
- [80] L. Qin, D. Huang, P. Xu, G. Zeng, C. Lai, Y. Fu, H. Yi, B. Li, C. Zhang, M. Cheng, C. Zhou, X. Wen, In-situ deposition of gold nanoparticles onto polydopamine-decorated g-C<sub>3</sub>N<sub>4</sub> for highly efficient reduction of nitroaromatics in environmental water purification, *J. Colloid Interface Sci.* 534 (2019) 357–369.
- [81] J. Wang, X.-B. Zhang, Z.-L. Wang, L.-M. Wang, W. Xing, X. Liu, One-step and rapid synthesis of “clean” and monodisperse dendritic Pt nanoparticles and their high performance toward methanol oxidation and p-nitrophenol reduction, *Nanoscale* 4 (2012) 1549–1552.
- [82] S. Altunçik, S. Koyuncu, A novel viologen-derived covalent organic framework based metal free catalyst for nitrophenol reduction, *ChemCatChem* 15 (4) (2023), e202201418.
- [83] A.N. Alqhobisi, M.S. Alhumaimess, I.H. Alsohaimi, H.M.A. Hassan, A.A. Essawy, M.R. El-Aassar, H. Kalil, Efficient nitrophenol reduction with Noria-GO nanocomposite decorated with Pd-Cu nanoparticles, *Environ. Res.* 231 (2023), 116259.
- [84] M. Banou, Y. Niu, F. Ammari, T. Dunlop, R.E. Palmer, C. Tizaoui, Fabrication of graphene nanoplatelets/MgAl-layered double hydroxide nanocomposites as efficient support for gold nanoparticles and their catalytic performance in 4-nitrophenol reduction, *Process Saf. Environ. Protect.* 174 (2023) 891–900.
- [85] A. Ismail, M.A.K. Alsouz, H.A. Almashhadani, M.F. Khan, M. Zahid, An efficient Ag decorated CeO<sub>2</sub> synergetic catalyst for improved catalytic reduction of lethal 4-nitrophenol, *Chem. Phys. Impact* 6 (2023), 100173.
- [86] W. Yu, L. Qiu, J. Zhu, S. Chen, S. Song, Fe-embedded ZIF-derived N-doped carbon nanoparticles for enhanced selective reduction of p-nitrophenol, *J. Environ. Chem. Eng.* 11 (2023), 109609.
- [87] L. Tan, X. Liu, Y. Zhang, Glutaraldehyde fixation promotes palladium and gold nanoparticles formation in yeast and enhances their catalytic activity in 4-nitrophenol reduction, *J. Hazard Mater.* 446 (2023), 130696.

- [88] F. Wei, M. Luo, J. Lan, F. Xie, L. Cai, T.-S. Chan, M. Peng, Y. Tan, Pd atomic engineering of nanoporous Ni/NiO for efficient nitrophenol hydrogenation reaction, *ACS Appl. Mater. Interfaces* 15 (22) (2023) 26746–26754.
- [89] N.J. Mondal, R. Sonkar, S. Thakur, N.Ch Adhikary, D. Chowdhury, Structural modification in Au-MoS<sub>2</sub> quantum dot composites for improved catalytic efficiency in p-nitrophenol reduction, *ACS Appl. Nano Mater.* 6 (9) (2023) 7351–7363.
- [90] S.A. Manafi, B. Yazdani, M.R. Rahimiopour, S.K. Sadrnezhad, M.H. Amin, M. Razavi, Synthesis of nano-hydroxyapatite under a sonochemical/hydrothermal condition, *Biomed. Mater.* 3 (2008), 025002.
- [91] Y. Karatas, M. Yurderi, M. Gulcan, M. Zahmakiran, M. Kaya, Palladium (0) nanoparticles supported on hydroxyapatite nanospheres: active, long-lived, and reusable nanocatalyst for hydrogen generation from the dehydrogenation of aqueous ammonia–borane solution, *J. Nanoparticle Res.* 16 (2014) 2547.
- [92] J.E. Hutchison, G.H. Woehrie, S. Özkar, R.G. Finke, Analysis of nanoparticle transmission electron microscopy data using a public-domain image-processing program, *Image, Turk. J. Chem.* 30 (2006) 1–13.
- [93] Y. Karatas, A. Zengin, M. Gülcan, Preparation and characterization of amineterminated delafossite type oxide, CuMnO<sub>2</sub>-NH<sub>2</sub>, supported Pd (0) nanoparticles for the H<sub>2</sub> generation from the methanolysis of ammonia-borane, *Int. J. Hydrogen Energy* 47 (2022) 16036–16046.
- [94] M. Gulcan, Mehmet Zahmakiran, S. Özkar, Palladium (0) nanoparticles supported on metal organic framework as highly active and reusable nanocatalyst in dehydrogenation of dimethylamine-borane, *Appl. Catal. B Environ.* 147 (2014) 394–401.
- [95] Y. Karatas, M. Gülcan, M. Çelebi, M. Zahmakiran, Pd (0) nanoparticles decorated on graphene nanosheets (GNS): synthesis, definition and testing of the catalytic performance in the methanolysis of ammonia borane at room conditions, *ChemistrySelect* 2 (2017) 9628–9635.
- [96] S.J. Greg, K.S.W. Sing, Adsorption, Surface Area, and Porosity, Academic Press, New York, 1997.
- [97] K.K. Senapati, S. Roy, C. Borgohain, P. Phukan, Palladium nanoparticle supported on cobalt ferrite: an efficient magnetically separable catalyst for ligand free Suzuki coupling, *J. Mol. Catal. Chem.* 352 (2012) 128–134.
- [98] S. Pai, M.S. Kini, R. Selvaraj, A review on adsorptive removal of dyes from wastewater by hydroxyapatite nanocomposites, *Environ. Sci. Pollut. Res.* 28 (2021) 11835–11849.
- [99] K.A. Connors, *Theory of Chemical Kinetics*, VCH Publishers, New York, 1990.
- [100] M.V. Twigg, *Mechanisms of Inorganic and Organometallic Reactions*, Plenum Press, New York, 1994.